Concurrent Observation of Bulk and Protein Hydration Water by Spin-Label ESR under Nanoconfinement

ARTICLE *in* LANGMUIR · OCTOBER 2013

Impact Factor: 4.46 · DOI: 10.1021/la403002t · Source: PubMed

3 AUTHORS, INCLUDING:

Kuo Yun-Hsuan
National Tsing Hua University
2 PUBLICATIONS **4** CITATIONS

SEE PROFILE

Yun-Wei Chiang
National Tsing Hua University
27 PUBLICATIONS **482** CITATIONS

SEE PROFILE

Langmuir

Article

pubs.acs.org/Langmuir

Concurrent Observation of Bulk and Protein Hydration Water by Spin-Label ESR under Nanoconfinement

Yun-Hsuan Kuo, Yu-Ru Tseng, and Yun-Wei Chiang*

Department of Chemistry and Frontier Research Center on Fundamental and Applied Sciences of Matters, National Tsing Hua University, Hsinchu 30013, Taiwan

Supporting Information

ABSTRACT: Under nanoconfinement the formation of crystalline ice is suppressed, allowing the study of water dynamics at subfreezing temperatures. Here we report a temperature-dependent investigation (170−260 K) of the behavior of hydration water under nanoconfinement by ESR techniques. A 26-mer-long peptide and the Bax protein are studied. This study provides site-specific information about the different local hydrations concurrently present in the protein/peptide solution, enabling a decent comparison of the hydration molecules—those that are buried inside, in contact with, and detached from the protein surface. Such a comparison is not possible without employing ESR under nanoconfinement. Though the confined bulk and surface hydrations behave differently, they both possess a transition similar to the reported fragile-to-strong crossover transition around 220 K. On the contrary, this transition is absent for the hydration near the buried sites of the protein. The activation energy determined under nanoconfinement is found to be lower in surface hydration than in bulk hydration. The protein structural flexibility, derived from the interspin distance distributions $P(r)$ at different temperatures, is obtained by dipolar ESR spectroscopy. The $P(r)$ result demonstrates that the structural flexibility is strongly correlated with the transition in the surface water, corroborating the origin of the protein dynamical transition at subfreezing temperatures.

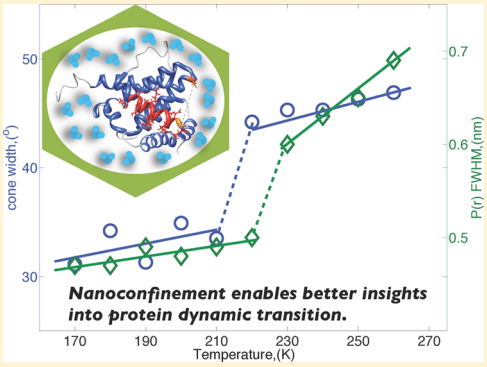

INTRODUCTION

When the dynamical properties of many proteins are plotted as a function of temperature, a biphasic behavior is often observed with a transition around 220 K,[1−3] known as the universal protein dynamical transition, although other dynamical transition temperatures ranging from 110 to 250 K have also been reported elsewhere.[3−6] The transition of the hydration shells and the protein itself is yet to be resolved. The dynamical transition is in many of the studies, observed for the hydration water on protein under a partial hydration level (to retain water on the surface solely),[1,3] i.e., the so-called hydrated protein powders, and is thought to be the fragile-to-strong dynamic crossover (FSC) around 220 K, similar to that observed in confined bulk water in silica nanochannels.[7−10] In reality, a functional protein is surrounded by few hydration shells and is embedded in a bulk excess solvent. Protein dynamics is not only coupled to motions of the surface hydration but is also to some extent influenced by the bulk solvent.[11] However, observation of the FSC for protein surface hydration in a fully hydrated state has been extremely difficult as water crystallizes in the presence of bulk hydration at subfreezing temperatures. Recently, it has been reported by electron spin resonance (ESR) technique that biomolecules in the absence of cryoprotectants could retain their conformations at cryogenic temperatures when confined in nanochannels, in which the formation of ice is suppressed.[12,13] Here we employ ESR under nanoconfinement to overcome the difficulty, unraveling new insights into the protein dynamical transition.

The FSC transition temperature of hydration water is defined as follows. At high temperatures, average rotational correlation time (τ_R) adheres to a super-Arrhenius behavior describable by a Vogel−Fulcher−Tammann (VFT) law, i.e., $\tau_R = \tau_0 \exp(DT_0/(T - T_0))$, where D is a constant related to fragility and T_0 is the ideal glass transition temperature at which the correlation time appears to diverge. In reality, this divergence would not happen in water. An Arrhenius behavior sets in below the crossover temperature T_L. The dependence of the τ_R on temperature follows a law, $\tau_R = \tau_0 \exp(E_A/k_BT)$, where k_B is the Boltzmann constant and E_A is the activation energy for the molecular relaxation process. Therefore, the crossover temperature T_L is determined by the intersection of the two equations. The transition from the super-Arrhenius to Arrhenius behaviors is the so-called fragile-to-strong crossover.

Water molecules interact with protein strongly. Protein dynamics may be correlated with (at least) three types of water in a protein solution: (i) the internal water, (ii) the surface hydration water, and (iii) the bulk water. Identification of their respective interactions to the protein is of utmost relevance to the understanding of protein dynamics. Here we demonstrate,

Received: August 4, 2013
Revised: October 18, 2013
Published: October 18, 2013

through an experiment combining site-directed spin-labeling ESR (SDSL-ESR) technique with nanochannels,[12−14] that the dynamics of the three types of water molecules can be identified and characterized in the temperature range between 170 and 260 K. In spin-label ESR, the introduction of a paramagnetic nitroxide side chain is accomplished through cysteine-substitution mutagenesis without a limitation in molecular size, sample types, and morphologies.[15,16] Thus, it has been demonstrated as a powerful tool for studying protein conformations and dynamics. ESR provides several unique features for systematically investigating protein−solvent dynamics in full hydration. It provides site-specific information about the local environment to which the spin label is attached. With a pair of spin labels attached to a protein, it allows the determination of interspin distances and distance distributions, providing an estimate of the structural flexibility of the protein at specific temperatures and hydration conditions and, as a result, enabling a better separation of the protein structural flexibility from the local hydration dynamics. ESR spectral line shape is extremely sensitive to a molecular motion and dynamics within the slow-motional regime, which corresponds to a rotational correlation time approximately within the micro- and nanosecond regime. Using the rigorous theoretical methods developed by Freed and co-workers, it is possible to interpret the spectral line shapes in terms of the relevant spin parameters to learn about the dynamics of the molecular reorientational process, providing specific information about local environment.[17,18] In the aspects of water dynamics study, the ESR technique has been demonstrated to be highly sensitive to the dynamics of hyperquenched glassy or supercooled water within temperature range 150−235 K,[19,20] also known as "no man's land" (NML).[21] It is therefore demonstrated that, at temperatures within the NML, the dynamics of spin label is coupled with local hydration dynamics.

In the present study, the dynamics of confined bulk water is probed by a nitroxide radical doped in pure water and is found to possess a transition around 220 K, which resembles the FSC reported for confined water. A 26-mer-long peptide exhibiting a simple β-hairpin structure in pure water is spin-labeled and studied under nanoconfinement to avoid the formation of ice crystal.[13] This peptide is used to investigate hydration dynamics near the spin-labeled site, providing site-specific information about the local hydration environment. The surface hydration of the peptide is also found to possess an FSC-like transition similar to that of confined bulk water. An approach that allows the concurrent observation of the bulk and surface hydrations is thus demonstrated. Moreover, this study investigates several solvent-exposed and buried sites on a B-cell lymphoma 2 Associated X (Bax)[22] protein under nanoconfinement at temperatures 170−260 K. A transition similar to the FSC of the peptide surface is observed for the solvent-exposed sites but is absent at the buried sites of the Bax. The findings in this study lead to a clear discrimination in dynamics among internal hydration, protein surface hydration, and bulk water as confined in nanochannels.

By way of introduction, we note an underlying principle of this study below. The employed nitroxide spin label, as attached to a protein, is in close vicinity (<0.7 nm in side chain length) to the protein surface; as such, its dynamical change naturally correlates with the dynamics of the surrounding solvent molecules. This is a reasonable assumption as the tumbling motion of spin-labeled biomolecules was verified, even at room temperature, to become too slow to dominate the spectral line shape under nanoconfinements.[23] Moreover, at subfreezing temperatures, inhomogeneous broadening (IB) due to unresolved nearby protons could become comparable to the spectral changes caused by the local dynamics of the spin probe. This study uses deuterated solvents and spin labels to reduce this unwanted IB effect, enhancing the spectroscopic sensitivity to the slow hydration dynamics at low temperatures and under nanoconfinements. Therefore, the local hydration surrounding the spin label is herein considered akin to the local hydration at the surface of the peptide/protein, thereby being referred to as surface hydration, with stipulations that (i) it covers largely the first few layers of hydration water in immediate proximity to the protein/peptide surface and (ii) it may not necessarily be a surface-coupled hydration that has an attraction/repulsion to the surface.

EXPERIMENTAL SECTION

Materials and Sample Preparation. Nitroxide-based spin probes (4-hydroxy-2,2,6,6-tetramethylpiperidine-1-oxyl, TEMPOL, and per-deuterated TEMPOL, PD-TEMPOL) and deuterated glycerol were purchased from Sigama-Aldrich, Inc. The mesoporous silica SBA15 materials were purchased from ACS Material, LLC, with an average pore diameter of 7.6 nm and unit cell size of 11.6 nm. This nanochannel was previously demonstrated useful for confining biomolecules in ESR study.[12,24] The n3 peptide was custom-synthesized by Kelowna International Scientific Inc. (New Taipei, Taiwan) with purity greater than 95%. The n3 peptide is a linear 26-mer-long model polypeptide carrying a cysteine at the ninth residue for conjugating with a nitroxide spin probe. The spin-labeled n3 peptide is denoted by n3-R1. This model peptide has been extensively studied by NMR and ESR and found to display a β-hairpin conformation in pure water when confined in the nanochannels.[12] For the preparation of lyophilized sample, the solution sample was dialyzed against two changes of 1 L distilled water for 1 h each and another 1 L distilled water overnight. After dialysis the sample was loaded into a 4 mm EPR tube and frozen in liquid nitrogen prior to sending to freeze-drier (EYELA FDU-1200) at a pressure of approximately 10 Pa and a condenser temperature of −50 °C for at least 24 h.

Protein Expression and Purification. Unless specified otherwise, all chemicals used in the Bax study were from Sigma-Aldrich, Inc. The cDNA of mouse Bax was subcloned into NdeI/SapI site of pTYB1vector (New England Biolabs, Inc.). The mutant constructs were generated by using a QuikChange mutagenesis kit (Stratagene), and the nucleotide sequences were confirmed by sequencing. We followed the same procedure as previously described.[25] The pTYB1-Bax construct encoding a fusion protein of Bax with chitin binding peptide was separated by a self-cleavable intein tag to obtain a full-length Bax. All proteins were expressed *Escherichia coli* ER2566 strain and purified without adding detergent. Bacterial cultures were grown at 37 °C in LB medium containing ampicillin (0.1 g/L) to reach an OD_{600} of 0.6−0.8. Protein expression was induced by addition of 0.3 mM of IPTG (isopropyl 1-thio-β-D-galactopyranoside) at 30 °C for 4−6 h. The cell pellet was collected by centrifugation and resuspended in ice-cold lysis buffer (20 mM Tris-HCl, pH 8.0, 500 mM NaCl and 1 mM PMSF), followed by lysing pellet with sonication. The insoluble pellet was removed twice by centrifugation at 10 000 rpm for 40 min at 4 °C, and the clear supernatant containing Bax protein was loaded onto chitin affinity resin column at a flow rate about 0.5−1 mL/min at 4 °C. Resin was subjected to a high salt (20 mM Tris-HCl, pH 8.0, 2 M NaCl) wash and then incubated in equilibrated buffer (20 mM Tris-HCl, pH 8.0, 100 mM NaH_2PO_4, 60 mM dithiothreitol) for 16−48 h at 4 °C. Protein was purified by a size exclusion chromatography using a HiLoad 16/60 Superdex 75 column (GE Healthcare). The purified protein was confirmed by SDS-PAGE with Coomassie blue staining and Western blot, and the protein concentration was estimated using a BioPhotometer by measuring absorbance at 280 nm. The proteins

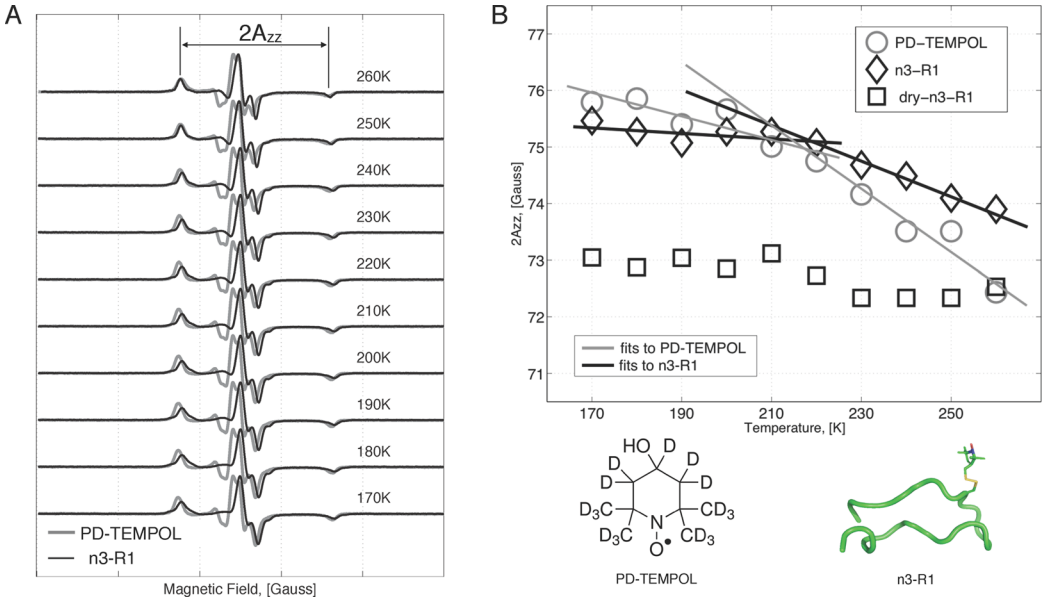

Figure 1. (A) CW-ESR spectra of PD-TEMPOL (gray) versus n3-R1 (black) as confined in D_2O-filled SBA15 nanochannels at temperatures 170−260 K. The parameter $2A_{zz}$ is indicated in the spectrum. Under the same experimental condition, the spectra of the two samples differ substantially, indicating two distinct local environments. (B) The $2A_{zz}$ parameter as a function of temperature for the samples, PD-TEMPOL, n3-R1, and dry-n3-R1. Straight lines are least-squares fits to the data. The error in the measurements below 200 K is ±0.4 G; above 200 K it decreases to ±0.2 G. The structure of PD-TEMPOL and the cartoon model of n3-R1 are provided.

were labeled with a 10-fold excess of (1-oxy-2,2,5,5-tetramethyl-3-pyrroline-3-methyl)methanethiosulfonate spin label (MTSL) (Alexis Biochemicals, San Diego, CA) per cysteine residue for overnight in the dark at 4 °C. To remove free radicals, the spin-labeled Bax solution was dialyzed against 4 changes of buffer A (20 mM sodium phosphate, pH 8.0, 100 mM NaCl) over 1−3 h and final change of buffer over 24 h. The volume of the buffer is about 1000 times that of the protein solution.

Experimental Procedures. In the spin-labeling experiment, peptides/proteins were labeled with a 10-fold excess of MTSL per cysteine residue for overnight in the dark at 4 °C. Peptides were further purified by reverse phase HPLC. MALDI-TOF experiments were conducted to confirm the identity of the peptides/proteins carrying the spin labels. The solution volume added into an ESR tube for the bulk solution studies was ca. 40 μL. The encapsulation of the peptide samples into the nanochannels was prepared following the previously developed protocol,[12,13] where the n3-R1 was shown to retain its structure in the SBA15 nanochannels. The solution volume added onto the nanochannels (0.1 mL, 12 mg) was ca. 20 μL. No cryoprotectant was used for the nanochannel experiments. The deuterium−hydrogen exchange experiment to modify the surface group of the nanochannel materials was performed as previously described.[12] The concentration of the spin-labeled peptides/proteins was 0.3−0.5 mM. In the bulk solution studies concerning Bax protein, two cryoprotectants (ficoll and glycerol) were used as noted in text. The encapsulation of the Bax protein into the nanochannels was the same as the procedure for the n3-R1 peptide. We performed the following experiments to verify that the spin-labeled peptides/proteins were not adsorbed/left on the outer surface of the materials and that the molecules were trapped adequately well within the nanochannels. An excess buffer was added into the ESR tube containing the mesoporous materials. The tube was sent for ESR measurements at room temperature. The collected spectra were found to remain identical to the spectra collected before the addition of the excess buffer; that is, the spectra show typical slow-motional line shapes, indicating the presence of the nanoconfinement effect. This study also confirmed that no ESR signal was obtained for the supernatant liquid after centrifugation. Strong ESR signals were detected in the supernatant liquid after the materials were incubated in excess buffer for longer than 2 weeks. Figure S1 shows the spectra of circular dichroism (CD) for spin-labeled Bax at 25 °C. The CD spectra obtained in the presence versus absence of nanochannels are similar and characterized with the same peaks, showing a strong propensity for helical structures as expected for the Bax. Taken together with the $2A_{zz}$ polarity data (cf. Results), it indicates that the structure of Bax remains approximately unchanged upon the encapsulation into the nanochannels.

CW-ESR Measurements. A Bruker ELEXSYS E580 CW/pulsed spectrometer was used. The ESR experiment was performed at an operating frequency of 9.4 GHz and 1.5 mW incident microwave power. The swept magnetic range was 200 G. ESR probehead was precooled to 170 K prior to the transfer of the ESR sample tube into the cavity. The same spectra were obtained if the tube was plunge-cooled in liquid nitrogen prior to the transfer. Equilibrium time was 20 min for each temperature variation. Each experiment was repeated two to four times to estimate the errors in the A_{zz} values. Though the measurement error (e.g., ±0.3−0.4 G in Results) was sufficiently small, it would result in a seemingly large variation in the τ_R (as A_{zz} approaches A_{zz0} at low temperatures) due to that the value of $(1 - A_{zz}/A_{zz0})$ becomes comparable to experimental uncertainties as the spectrum approaches the rigid limit.

RESULTS

In Figure 1A, the spectra in gray and black were obtained for PD-TEMPOL and n3-R1, respectively, as the samples were confined in D_2O-filled SBA15 nanochannels at 170−260 K. The PD-TEMPOL is a small radical, and the n3-R1 is a relatively large spin-labeled (26-mer-long) polypeptide. See Experimental Section for details and Figure 1 for their structures. The silanol groups on surface of the nanochannels were deuterated prior to the measurements. It clearly shows in Figure 1A that the spectra for the two samples (PD-TEMPOL versus n3-R1) differ substantially at the same temperature and that they exhibit typical very-slow-motional line shapes, indicating that the studied molecules are strongly confined in the nanochannels. As illustrated in Figure 1A, the parameter $2A_{zz}$, i.e., the splitting between the outer hyperfine peaks, is used to represent changes in the local environment concerning

dx.doi.org/10.1021/la403002t | Langmuir 2013, 29, 13865−13872

temperature. Namely, the $2A_{zz}$ reflects the changes of the spin-label motion caused by the changes in the local hydration state. Details about the hydration-modulated spectral changes are given in the Discussion. In Figure 1B, the parameter $2A_{zz}$ from the CW-ESR spectra is plotted as a function of temperature for the studied samples. Gray circles and black diamonds represent the data obtained for PD-TEMPOL and n3-R1, respectively, in D_2O-filled nanochannels, while black squares stand for the data obtained for lyophilized n3-R1 (denoted by dry-n3-R1, whose spectra are shown in Figure S2). The results clearly display differences in the temperature-dependent $2A_{zz}$ variation for the three samples. For the two hydrated samples under nano-confinement, a decrease in $2A_{zz}$ was observed with an increase in temperature, with PD-TEMPOL having a lower $2A_{zz}$ value for temperatures (approximately) above 220 K and a higher $2A_{zz}$ value below 220 K. The solid lines in gray and black represent the first-order polynomial fits to the $2A_{zz}$ measurements for the PD-TEMPOL and n3-R1, respectively. To obtain the best possible fit, two straight lines were required for each of the hydrated samples: one for temperatures below 220 K and the other for temperatures above 220 K. However, the behavior of the two hydrated samples is clearly different within the same temperature region, as indicated by the different rates by which the $2A_{zz}$ changes with temperature. For the dry-n3-R1 sample the variation of the $2A_{zz}$ with temperature is much smaller than those for the hydrated samples. The data for the dry-n3-R1 can be easily fitted using a straight line with a small slope, showing no indication of the transition as observed in the hydrated samples. Evidently, the results in Figure 1 indicate that (i) the presence of the surface hydration is required for the observation of the transition using the $2A_{zz}$ data, (ii) there is a transition around 220 K for the two hydrated samples under nano-confinement, and (iii) there are two hydrations, in which their dependencies with temperature are clearly different. Below we demonstrate that the observed two hydrations (local environments) coexist within the NML in the nanochannel.

Figure 2 shows the experimental spectra (in gray) obtained from a mixture of PD-TEMPOL and n3-R1 samples encapsulated in D_2O-filled nanochannels, while the spectra in black is a least-squares fit to the experimental spectra by a linear combination of the respective spectra (shown in Figure 1A) of PD-TEMPOL and n3-R1 at a same temperature. The simulated spectra fit well with the experimental data with respective populations of 50 ± 2%. This indicates that the local environments of the two samples coexist in the nanochannels, suggesting the coexistence of confined bulk water (reported by PD-TEMPOL) and peptide surface water (reported specifically by the attached spin label) in the studied conditions. Such a concurrent observation of the two hydrations under nano-confinement within the NML has never been reported. Besides, the result indicates that the two samples are homogeneously dispersed and adequately separated from each other in the nanochannels, as line width broadening, which is often caused by the spin−spin coupling in distances <2 nm, is not observed at all in the spectra of the mixture samples.

As the spectra obtained within the NML belong to the very slow-motional regime of the ESR time scale, the A_{zz} values can be used to yield the ensemble rotational correlation time τ_R with eq 1[17]

$$\tau_R = \alpha(1 - A_{zz}/A_{zz0})^{\beta} \quad (1)$$

where A_{zz0} is one-half the separation of the outer hyperfine extrema in the rigid limit condition, and the model parameters

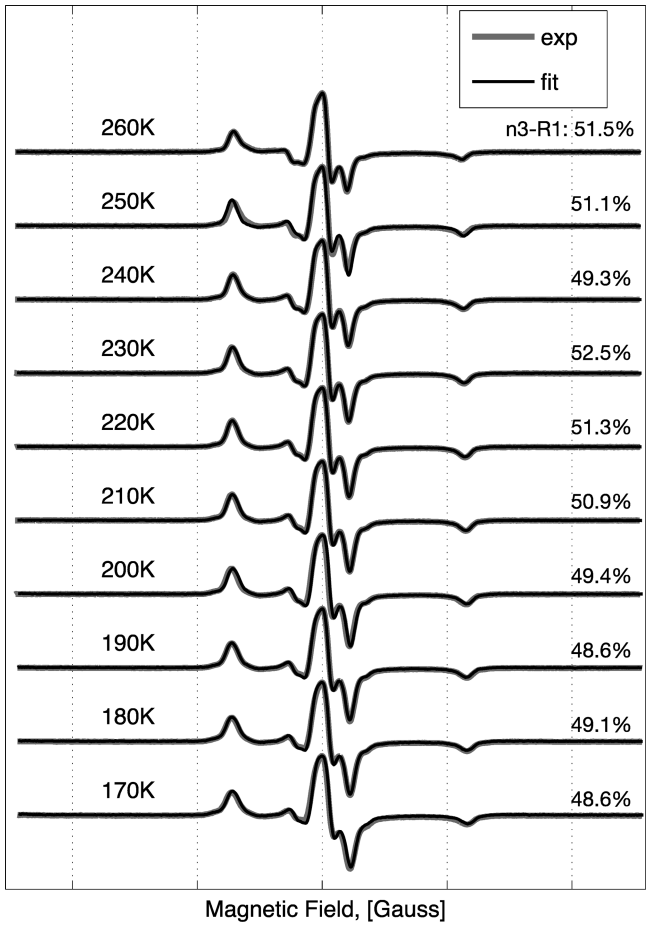

Figure 2. CW-ESR spectra (denoted by gray lines) obtained as PD-TEMPOL and n3-R1 are both confined in the D_2O-filled nanochannels. The spectra are shown in a normalized format. The fits to the spectra in gray lines are generated by a linear combination of the two respective individual spectra (cf. Figure 1A) at the sample temperature. The population of n3-R1 is indicated. A very good quality of the fits to the gray lines is achieved. This experiment demonstrates that (i) the two distinctly different local environments (suggested in Figure 1A) coexist in the nanochannel and (ii) the two samples are adequately separated (>2 nm) from each other in the nanochannel.

α and β are 2.57×10^{-10} s and −1.78, respectively, which are determined by the rigorous theory of Freed and co-workers.[17] In Figure 3, the calculated τ_R values for the two samples of PD-TEMPOL (by gray circles) and n3-R1 (by black diamonds) are plotted as a function of $1/T$ in a log−linear plot. The theoretical analysis shows that there is a distinct transition from a VFT law at high temperatures to an Arrhenius law at low temperatures in the two samples, with the fitted crossover temperature T_L between 210 and 220 K, the ideal glass transition temperature $T_0 \approx 150$ K, and the activation energy E_A approximately 0.91 kcal/mol (n3-R1) and 1.72 kcal/mol (PD-TEMPOL). In the temperature range 220−260 K, the average τ_R obeys a VFT law, displaying a signature of a fragile state, whereas upon crossing over temperatures around the T_L it suddenly switches to an Arrhenius law, a signature of a strong state. Therefore, we have a clear evidence for the FSC transition in a cusp curve.

Figure 4A shows a cartoon model of the Bax protein and residues 64 and 72, which are mostly solvent-exposed as suggested by the NMR structure (PDB: 1F16), and residues 63 and 67, which are mostly buried on the structure. The four Bax

dx.doi.org/10.1021/la403002t | Langmuir 2013, 29, 13865−13872

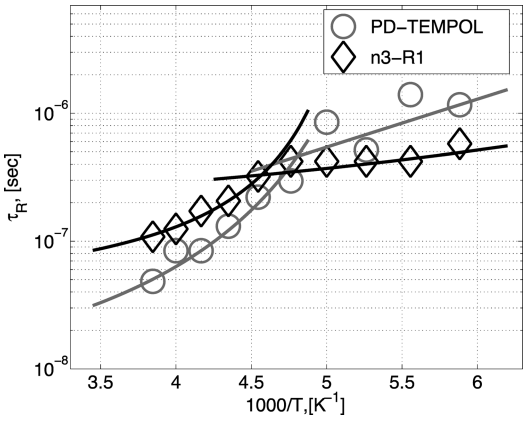

Figure 3. The log–linear plot of the τ_R vs $1/T$ for the PD-TEMPOL and n3-R1 samples and the theoretical fits (solid lines) to the data points. The ideal glass transition temperature T_0 = 150 K is used. There is a clear transition (T_L approximately 210–220 K) from a VFT law at high temperatures to an Arrhenius law at low temperatures. This analysis demonstrates that under nanoconfinement the FSC transition occurs in both the bulk water (reported by PD-TEMPOL) and the peptide surface hydration (reported by the attached spin probe).

mutants were prepared for spin-labeling, each carrying one cysteine, which was to be conjugated with the MTSL probe to form a R1 side chain. The spectra obtained for the four spin-labeled Bax proteins confined in SBA15 nanochannels at 170–260 K are shown in Figure S3, while its corresponding $2A_{zz}$ versus T plot is shown in Figure 4B. The $2A_{zz}$ for the spectra of the Bax64R1 and Bax72R1 was found to decrease with increasing temperature and vary in a trend quite similar to what was observed for the n3-R1 study shown in Figure 1B. Interestingly, the $2A_{zz}$ of the two buried sites (Bax63R1 and Bax67R1) was found to increase with T, showing a trend completely different from the results of the solvent-exposed sites.

Moreover, the Bax proteins were also studied in vitrified bulk solvents. The spectra for the four spin-labeled Bax proteins in a vitrified bulk solvent containing 40% (w/w) ficoll are shown in Figure S4, while the spectra for the solvent containing 40% (v/v) glycerol are shown in Figure S5. The corresponding plots for $2A_{zz}$ versus T are shown in Figures 4C and 4D. The changes observed for the $2A_{zz}$ with T in the two vitrified bulk solvents are clearly subtle as compared to the changes for the nanochannel study (cf. Figure 4B), indicating that in the two vitrified bulk solvents the local hydration dynamics of the Bax remains similar at different temperatures and the hydration is likely in an amorphous solid characterized by a long correlational time outside the ESR sensitivity time scale (nanoseconds to microseconds). Nanoconfinement is a key to the successful observation of hydration dynamics by ESR at low T. Although the spin probe is insensitive to the T-dependent local dynamics in the bulk solvents, it is still useful to report the polarity of the local environment as revealed in the $2A_{zz}$ parameter. The $2A_{zz}$ values obtained for the solvent-exposed sites are greater than the values of the buried sites, as the greater the $2A_{zz}$, the greater extent the spin-labeled site is exposed to the solvent. This demonstrates that the tertiary

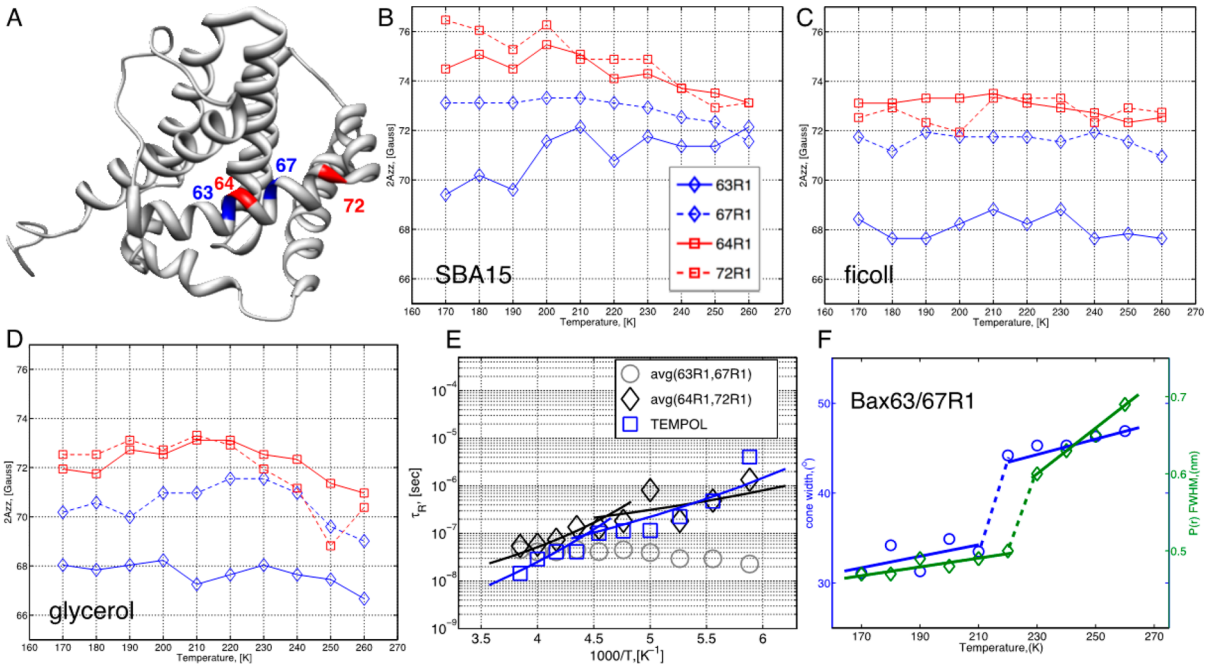

Figure 4. (A) A cartoon model of the Bax protein (PDB: 1F16) showing the four spin-labeled sites studied. The sites in red and blue represent the solvent-exposed and buried sites, respectively. The $2A_{zz}$ vs T plot for the spectra obtained in SBA15 is shown in (B). The $2A_{zz}$ vs T plots for the Bax in the vitrified bulk solvents containing ficoll and glycerol are shown in (C) and (D), respectively. Plots in (B–D) share the same legend given in (B). The error is about ±0.3 G. At T > 240 K, the global tumbling begins to take over the line shape changes due to the increased fluidity in (D). (E) The log–linear plot of the τ_R vs $1/T$ for the spin-labeled Bax proteins and TEMPOL probe. The plots show the respective averages of the buried sites (63R1 and 67R1) and the solvent-exposed sites (64R1 and 72R1). The black and blue solid lines are the theoretical fits to the data of the solvent-exposed sites and the data of TEMPOL, respectively. (F) The parameters (cone width and fwhm) derived from the distance measurements of the Bax63/67R1 reveal a transition around 210–220 K, which is related to the protein flexibility and is observed in the presence of the surface hydration.

dx.doi.org/10.1021/la403002t | *Langmuir* 2013, 29, 13865–13872

structure of the Bax protein is not disrupted in the studied bulk solvents.

To examine the impact of the surrounding hydration on the transition observed under nanoconfinement, dry (lyophilized) Bax was prepared to collect CW-ESR spectra in the absence of the hydration. The spectra of the lyophilized Bax are shown in Figure S6. The $2A_{zz}$ was found to hardly change with temperature (170−260 K), with fixed values of 69.8 ± 0.4 and 70.4 ± 0.4 G for Bax67R1 and Bax72R1, respectively, showing no abrupt changes that can imply a transition. Again, dry sample experiment verifies that the presence of surface hydration is required for observing the $2A_{zz}$ dependence with T.

In Figure 4E, we present the τ_R versus $1/T$ plot derived from the studied Bax proteins and TEMPOL as they were respectively confined in nanochannels. Note that protein buffer (i.e., the buffer A in Methods) rather than pure water was used in the experiments of Figure 4. The plots show the respective averages of the buried sites versus the solvent-exposed sites and, moreover, the result of TEMPOL. An FSC-like transition is observed for the results of the solvent-exposed sites on the Bax, at which the surface hydration is surely present (with $E_A \approx 2.31$ kcal/mol), and the TEMPOL study (with $E_A \approx 5.04$ kcal/mol), whereas the transition becomes absent in the data for the buried sites. (See Figure S7 for CW-ESR spectra of TEMPOL.) Taken together, this study is able to observe an FSC for confined bulk hydration, which is reported by TEMPOL or PD-TEMPOL, and for surface hydration in both the n3 and Bax studies. As demonstrated in the study of the lyophilized Bax that the surface hydration is required for the FSC transition to happen, the question remains to resolve is whether or not the protein dynamical transition is enslaved by the surface hydration. To probe the protein dynamics and concurrently minimize the influence of the surface hydration on the spin-label motion, this study performed the interspin distance measurements for Bax63/67R1, a doubly labeled Bax carrying spin labels at the two buried sites, at which the local hydration shows no indication of the FSC transition (cf. Figure 4E). The distance distribution $P(r)$ is determined in a tether-in-a-cone (TIAC)[26] theoretical analysis of the CW-ESR spectra. (See Supporting Information text and Figure S8 for details.) The parameters of the cone width of the side chain and the full width at half-maximum (fwhm) of the $P(r)$ concerning T are shown in Figure 4F. A clear transition is observed at 220 K. Both parameters (i.e., the fwhm and the cone width) decrease with decreasing temperature, while a drastic change is clearly observed around 220 K. This observation is consistent with the previous studies showing that proteins below T_L would exhibit a substantial reduction in structural flexibility.[1,2] As the dynamical changes in the local environments of the two buried sites are insignificant (cf. Figure 4E), we believe that the two parameters derived from the $P(r)$ reflect largely the protein structural flexibility transmitted from the dynamics of the surface hydration. Therefore, this TIAC study provides supporting evidence for the coupling of the protein dynamical transition and the surface hydration.

DISCUSSION

It was previously demonstrated that the SBA15 nanochannel is useful for reducing the tumbling motions of molecules while maintaining the target molecules in the slow-motional regime at room temperatures.[14,24] Accordingly, the local environment is better revealed at room temperatures than the conventional approach studied in bulk solution. In this study, we show that the studied molecules, though differ substantially in molecular size as comparing a PD-TEMPOL to a n3 peptide or a Bax protein, are strongly confined in the nanochannels so that only small residual line shape changes, which are responsive to local environment, are observed at subfreezing temperatures. All of the spectra in this study display typical slow-motional line shapes, making it easy to extract τ_R from the line shapes using the analysis method developed by Freed. The study of the dry samples verifies the strong coupling between the local hydration and the spin-label motion. Our result shows that under nanoconfinement within the NML molecular tumbling motions are too slow to dominate the line shape changes; as a result, it is the local structure changes of the hydration water, which consequently facilitate the motion of the spin label, thereby playing an important role in the line shape changes observed in the study. Supports to the above conclusion can be easily gained from the results and discussed below. Under the same nanoconfinement, the $2A_{zz}$ dependence with T (and, consequently, the E_A) for PD-TEMPOL and TEMPOL is distinctly different as the solution is changed from D_2O to protein buffer. This demonstrates that the ESR spectrum of this study is modulated by the T-dependent hydration dynamics rather than tumbling motion. Another support can be gained from the Bax study in the vitrified bulk solvent. Although the $2A_{zz}$ is rather robust in reflecting the local polarity distinguishing the buried sites from the solvent-exposed sites on Bax, it is insensitive to the temperature changes within the NML as the local viscosity is extremely high at low temperatures in the solvents. However, under nanoconfinement we can easily observe the $2A_{zz}$ changes with temperature for the Bax within the NML. Taken the Bax and n3-R1 results together, we show that the FSC can be observed in both cases regardless of molecular size. This indicates that the ESR spectra report the dynamics of protein surface hydration. Therefore, it is legitimate to say that the ESR spectra reflect largely the changes in local hydration dynamics. Moreover, the above observation rules out the possibility that the bulk/surface water in the SBA15 is solid, representing ESR evidence that the confined bulk and surface water molecules are noncrystalline within the NML. This is consistent with the findings[7,27] where nanoconfinement suppresses the formation of crystalline ice.

As demonstrated above, the employed spin probes have adequate sensitivity to the local hydration environment under nanoconfinement in the NML. This study has reported the evidence for concurrently observing the bulk and protein surface water in nanochannels. Previously such a concurrent observation for the two hydrations has been notoriously challenging, as without a site-specific probe it was impossible to distinguish the two hydrations at the same time. This previous experimental inability had made it impossible to carry out a suitable comparison for the two hydrations. In the present study, we show that in the nanochannels there exists two distinct and independent local environments, which represent the bulk and protein surface hydration, respectively, and that both the hydrations show FSC-like transition at $T_L \approx 220$ K. The estimated activation energy E_A required for the FSC to occur in the PD-TEMPOL study is approximately 2 times the E_A obtained for the n3-R1 study, suggesting a lower energy barrier in the n3 surface water than that in the confined bulk water. The surface effect appears to be a key to the E_A difference as the two samples were measured in the same experimental condition with D_2O as solvent. At temperatures above T_L it is reasonable to observe that PD-TEMPOL is

characterized by a shorter τ_R as compared to the τ_R of the n3-R1 (cf. Figure 3). A similar result was previously reported showing a modest slowdown of the surface hydration dynamics as compared to the bulk hydration,[11] whereas PD-TEMPOL (a small molecule as compared to the n3) is found to become longer in τ_R than the n3-R1 at temperatures below T_L. The result suggests that under nanoconfinement the local dynamics is higher (i.e., shorter τ_R) for the surface water than the bulk water at temperatures below T_L. The surface effect is indeed influential. The activation energy arises from the decrease in average free local volume available to the spin label as a result of the molecular ordering in the local hydration. This study suggests that the coupling between the local hydration (near the spin label) and surface is important; as such, it affects the dependence of τ_R on T, resulting in the E_A differences between bulk versus surface hydration water. This observation validates the underlying assumption (cf. Introduction) of the present study. Moreover, it is noteworthy that we were able to make the same observation for the studies of TEMPOL versus solvent-exposed sites of Bax as the solvent was protein buffer rather than pure water (cf. Figure 4E); the E_A of the former is found to be about 2 times the E_A obtained for the latter. The activation energy is consistently found to be higher for confined bulk solvent than protein/peptide surface hydration under nanoconfinement. To the best of our knowledge, E_A values of bulk water and protein surface hydration have never been measured concurrently under nanoconfinement and reported in literature. Some relevant studies by quasi-elastic neutron scattering (QENS) are taken together and given below. It was reported that E_A determined for water in nanochannels[7] is higher as compared to that of hydrated protein surface[1] (without nanochannels). A recent QENS study also showed that under nanoconfinement monolayer water is slower than full hydration water at high temperatures but faster at low temperatures within the NML. All of these studies support the finding of the present study.

Another key feature of the present study is the identification of the three types of water by the SDSL technique. While the bulk and surface water have been extensively investigated in the literature, study about the internal water has been scarcely reported. With the SDSL-ESR approach, our result for the buried sites on Bax shows that (i) it features a local polarity distinctly less than that for the solvent-exposed sites and (ii) its A_{zz} dependence with T is completely different from that for the solvent-exposed sites; moreover, its corresponding τ_R shows no indication of the FSC transition. Making use of this feature of the buried sites, we performed interspin distance measurements of the doubly labeled Bax protein at the buried sites. The obtained $P(r)$ is thus considered to represent largely the structural flexibility of the protein because the measurements were made in a condition where the influence of the local hydration dynamics is negligible and, at the same time, the protein surface hydration effect persists. Hence, we refer the transition observed in the $P(r)$ result to the surface-hydration-coupled protein dynamic transition. This transition coincides with the FSC transitions of bulk and surface hydrations around 220 K. This protein dynamics appears to couple with surface hydration. Lastly, we make a brief comment on the results of the buried sites. As the A_{zz} for the two buried sites (Figure 4B) under nanoconfinement show a different dependence with T, we believe that this is attributed to the differing extents of the hydrophobicity in the local environments (e.g., the internal hydrophobic hydration and the interactions with the nearby residues). A better model protein carrying an intact water cavity is expected to improve the consistency and is suggested for further investigations on the bound internal water using the combined approached of ESR and nanochannels. Besides, we expect that the study approach of suppressing ice crystal using nanochannels can also be combined with pulsed 2D-ESR techniques to better capture the dynamics of protein hydration.

SUMMARY

This study investigates the hydration dynamics, characterized by the nitroxide-based spin labels, of the bulk water, surface water, and internal water of the protein by SDSL-ESR experiments measured under nanoconfinement. It demonstrates that spin-label ESR technique is sufficiently sensitive to probe the dynamical changes and differences in bulk and surface hydrations at subfreezing temperatures. Also, this study reports an ESR evidence for the noncrystalline state of the confined bulk and surface water in the NML. The result shows that FSC is observed in all of the local hydration environments, by the spin probes, except for the hydration corresponding to the buried sites on the Bax protein, whereas FSC becomes absent as protein hydration is removed. A transition related to the protein structural flexibility is found to coincide with the FSC around 220 K and is demonstrated to correlate with the FSC of the surface hydration, implying that no real protein transition occurs around 220 K. All of these findings are not possible without the use of nanochannels for suppressing ice formation. This study provides evidence that under nanoconfinement the activation energy of bulk hydration is higher than that of protein/peptide surface hydration. These experiments can also provide a complement to other experiments by gaining site-specific information regarding the coupling of protein dynamics to the dynamics of the solvent.

ASSOCIATED CONTENT

Supporting Information

Supplementary methods and figures. This material is available free of charge via the Internet at http://pubs.acs.org.

AUTHOR INFORMATION

Corresponding Author

*E-mail: ywchiang@mx.nthu.edu.tw (Y.-W.C.).

Author Contributions

Y.W.C. designed the experimental plan, developed analytical tools, analyzed data, and wrote the paper. Y.H.K. and Y.L.T. developed experimental protocols and performed experiments. All the authors discussed the results and commented on the manuscript.

Notes

The authors declare no competing financial interest.

ACKNOWLEDGMENTS

This work was supported by the Taiwan NSC Grants NSC100-2113-M-007-013-MY2 and NSC102-2628-M-007-003-MY3. All of the CW/pulse ESR measurements were conducted in NSC Research Instrument Center of Taiwan located at NTHU.

REFERENCES

(1) Chen, S. H.; Liu, L.; Fratini, E.; Baglioni, P.; Faraone, A.; Mamontov, E. Observation of fragile-to-strong dynamic crossover in protein hydration water. *Proc. Natl. Acad. Sci. U. S. A.* **2006**, *103*, 9012−9016.

(2) Rasmussen, B. F.; Stock, A. M.; Ringe, D.; Petsko, G. A. Crystalline ribonuclease A loses function below the dynamic transition at 220 K. *Nature* **1992**, *357*, 423−424.
(3) Roh, J. H.; Novikov, V. N.; Gregory, R. B.; Curtis, J. E.; Chowdhuri, Z.; Sokolov, A. P. Onsets of anharmonicity in protein dynamics. *Phys. Rev. Lett.* **2005**, *95*, 038101.
(4) Kim, C. U.; Tate, M. W.; Gruner, S. M. Protein dynamical transition at 110 K. *Proc. Natl. Acad. Sci. U. S. A.* **2011**, *108*, 20897−20901.
(5) He, Y.; Ku, P. I.; Knab, J. R.; Chen, J. Y.; Markelz, A. G. Protein dynamical transition does not require protein structure. *Phys. Rev. Lett.* **2008**, *101*, 178103.
(6) Mazza, M. G.; Stokely, K.; Pagnotta, S. E.; Bruni, F.; Stanley, H. E.; Franzese, G. More than one dynamic crossover in protein hydration water. *Proc. Natl. Acad. Sci. U. S. A.* **2011**, *108*, 19873−19878.
(7) Faraone, A.; Liu, L.; Mou, C. Y.; Yen, C. W.; Chen, S. H. Fragile-to-strong liquid transition in deeply supercooled confined water. *J. Chem. Phys.* **2004**, *121*, 10843−10846.
(8) Xu, L. M.; Mallamace, F.; Yan, Z. Y.; Starr, F. W.; Buldyrev, S. V.; Stanley, H. E. Appearance of a fractional Stokes-Einstein relation in water and a structural interpretation of its onset. *Nat. Phys.* **2009**, *5*, 565−569.
(9) Liu, L.; Chen, S. H.; Faraone, A.; Yen, C. W.; Mou, C. Y. Pressure dependence of fragile-to-strong transition and a possible second critical point in supercooled confined water. *Phys. Rev. Lett.* **2005**, *95*, 117802.
(10) Mallamace, F.; Branca, C.; Corsaro, C.; Leone, N.; Spooren, J.; Stanley, H. E.; Chen, S. H. Dynamical crossover and breakdown of the Stokes-Einstein relation in confined water and in methanol-diluted bulk water. *J. Phys. Chem. B* **2010**, *114*, 1870−1878.
(11) King, J. T.; Kubarych, K. J. Site-specific coupling of hydration water and protein flexibility studied in solution with ultrafast 2D-IR spectroscopy. *J. Am. Chem. Soc.* **2012**, *134*, 18705−18712.
(12) Lai, Y. C.; Chen, Y. F.; Chiang, Y. W. ESR study of interfacial hydration layers of polypeptides in water-filled nanochannels and in vitrified bulk solvents. *PLoS One* **2013**, *8*, e68264.
(13) Huang, Y. W.; Lai, Y. C.; Tsai, C. J.; Chiang, Y. W. Mesopores provide an amorphous state suitable for studying biomolecular structures at cryogenic temperatures. *Proc. Natl. Acad. Sci. U. S. A.* **2011**, *108*, 14145−14150.
(14) Huang, Y. W.; Chiang, Y. W. Spin-label ESR with nanochannels to improve the study of backbone dynamics and structural conformations of polypeptides. *Phys. Chem. Chem. Phys.* **2011**, *13*, 17521−17531.
(15) Borbat, P. P.; Costa-Filho, A. J.; Earle, K. A.; Moscicki, J. K.; Freed, J. H. Electron spin resonance in studies of membranes and proteins. *Science* **2001**, *291*, 266−269.
(16) Fanucci, G. E.; Cafiso, D. S. Recent advances and applications of site-directed spin labeling. *Curr. Opin. Struct. Biol.* **2006**, *16*, 644−653.
(17) Goldman, S. A.; Freed, J. H.; Bruno, G. V. Estimating slow-motion rotational correlation times for nitroxides by electron-spin resonance. *J. Phys. Chem.* **1972**, *76*, 1858−1860.
(18) Schneider, D. J.; Freed, J. H., Calculating slow motional magnetic resonance spectra. A user's guide. In *Spin Labeling: Theory and Application*; Berliner, L. J., Reuben, J., Eds.; Plenum: New York, 1989; Vol. *8*, pp 1−76.
(19) Banerjee, D.; Bhat, S. N.; Bhat, S. V.; Leporini, D. ESR evidence for 2 coexisting liquid phases in deeply supercooled bulk water. *Proc. Natl. Acad. Sci. U. S. A.* **2009**, *106*, 11448−11453.
(20) Bhat, S. N.; Sharma, A.; Bhat, S. V. Vitrification and glass transition of water: Insights from spin probe ESR. *Phys. Rev. Lett.* **2005**, *95*, 235702.
(21) Mishima, O.; Stanley, H. E. The relationship between liquid, supercooled and glassy water. *Nature* **1998**, *396*, 329−335.
(22) Youle, R. J.; Strasser, A. The BCL-2 protein family: opposing activities that mediate cell death. *Nat. Rev. Mol. Cell Biol.* **2008**, *9*, 47−59.
(23) Sung, T. C.; Chiang, Y. W. Identification of complex dynamic modes on prion protein peptides using multifrequency ESR with mesoporous materials. *Phys. Chem. Chem. Phys.* **2010**, *12*, 13117−13125.
(24) Tsai, C. J.; Chiang, Y. W. Effects of anisotropic nanoconfinement on rotational dynamics of biomolecules: An electron spin resonance study. *J. Phys. Chem. C* **2012**, *116*, 19798−19806.
(25) Suzuki, M.; Youle, R. J.; Tjandra, N. Structure of Bax: coregulation of dimer formation and intracellular localization. *Cell* **2000**, *103*, 645−54.
(26) Hustedt, E. J.; Stein, R. A.; Sethaphong, L.; Brandon, S.; Zhou, Z.; DeSensi, S. C. Dipolar coupling between nitroxide spin labels: The development and application of a tether-in-a-cone model. *Biophys. J.* **2006**, *90*, 340−356.
(27) Kittaka, S.; Ueda, Y.; Fujisaki, F.; Iiyama, T.; Yamaguchi, T. Mechanism of freezing of water in contact with mesoporous silicas MCM-41, SBA-15 and SBA-16: Role of boundary water of pore outlets in freezing. *Phys. Chem. Chem. Phys.* **2011**, *13*, 17222−17233.

Supporting Information

Concurrent Observation of Bulk and Protein Hydration Water by Spin-label ESR Under Nanoconfinement

Yun-Hsuan Kuo, Yu-Ru Tseng, and Yun-Wei Chiang*

Department of Chemistry and Frontier Research Center on Fundamental and Applied Sciences of Matters, National Tsing Hua University, Hsinchu, 30013, Taiwan

*Correspondence E-mail: ywchiang@mx.nthu.edu.tw

METHODS

Determination of distance distributions by tether-in-a-cone (TIAC) model. The TIAC simulation program was kindly provided by Dr. Eric J. Hustedt and the analysis was performed as previously described.[1] Briefly, the TIAC model was incorporated into a computer software package designed for the nonlinear least squares analysis of ESR spectra. The best-fit parameters to the given spectra were obtained in a numerical analysis combining the simulated annealing and Marquardt-Levenberg algorithms. The TIAC model was developed for the simulation of cw-ESR spectra of dipole-dipole coupled nitroxide spin-labels attached to tethers statically disordered within cones of variable width. In this model, the nitroxides adopt a range of inter-spin distances and orientations, thereby allowing the determination of both the distance distribution and the relative orientation of the labels from experimental spectra. Previous simulations[1, 2] have demonstrated the sensitivity of ESR spectra to the orientation of the cones as a function of cone width and other parameters. The TIAC model was successfully used to analyze experimental spectra from T4 lysozyme.[1] These results demonstrated the utility of the model. In the theoretical analysis by the TIAC simulation, the nitroxides were placed at the end of tethers of length, 0.7 nm, which were separated by a distance of 0.68 nm, at their bases. The tethers adopted all possible angles within cones of width resulting in a distribution of inter-spin distances and orientations. The values used for the g- and A-tensors in the TIAC analysis were (2.0095, 2.0077, 2.0032) and (6.52, 5.83, 36.85), respectively.

(1) Hustedt, E. J.; Stein, R. A.; Sethaphong, L.; Brandon, S.; Zhou, Z.; DeSensi, S. C., Dipolar coupling between nitroxide spin labels: The development and application of a tether-in-a-cone model. *Biophys J* **2006,** *90*, 340-356.
(2) Hustedt, E. J.; Smirnov, A. I.; Laub, C. F.; Cobb, C. E.; Beth, A. H., Molecular distances from dipolar coupled spin-labels: the global analysis of multifrequency continuous wave electron paramagnetic resonance data. *Biophys J* **1997,** *72*, 1861-77.
(3) Tsai, C. J.; Chiang, Y. W., Effects of Anisotropic Nanoconfinement on Rotational Dynamics of Biomolecules: An Electron Spin Resonance Study. *J Phys Chem C* **2012,** *116*, 19798-19806.

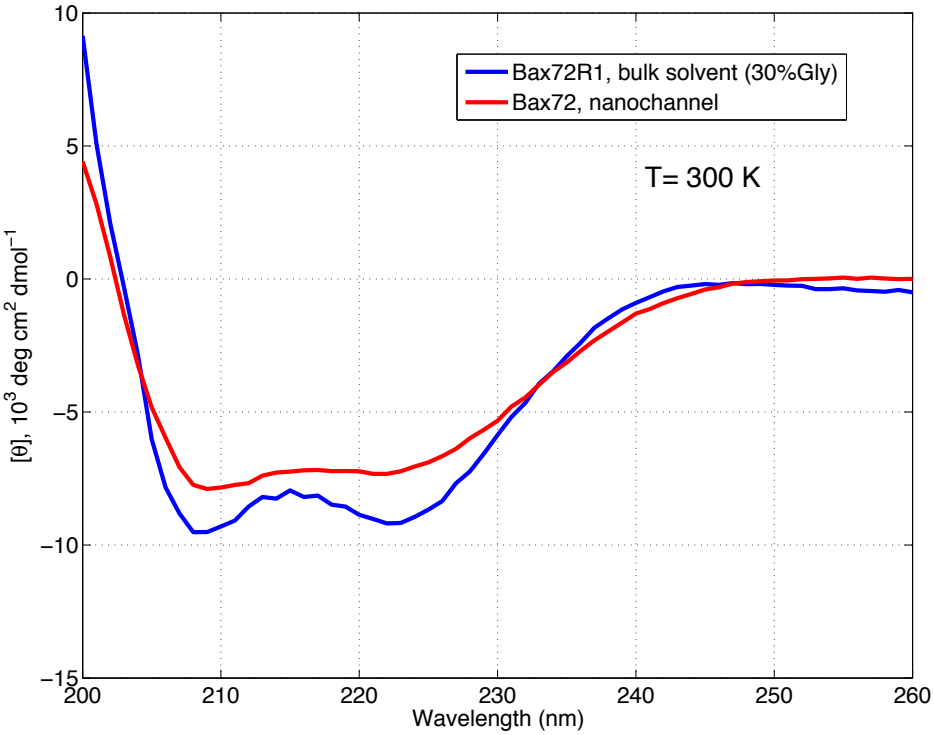

Figure S1. The CD spectra of Bax-72R1 in bulk solution (blue line) and within SBA15 nanochannels (red line) at 300 K. To obtain CD spectrum for a protein as confined in nanochannel, a previously published procedure was followed.[3] Briefly, nanochannel materials (4 mg) containing Bax proteins were dispersed within 0.4 mL of pure glycerol in a 1 mm CD cell. The CD spectra of the Bax in the bulk solvent versus within the nanochannels were verified to be similar, both of which possessed the same negative characteristic peaks around 208 and 222 nm that were indicative of a helix-rich Bax structure. The similarity of the two spectra indicates the secondary structure of the Bax remains approximately unchanged upon encapsulation into the nanochannel.

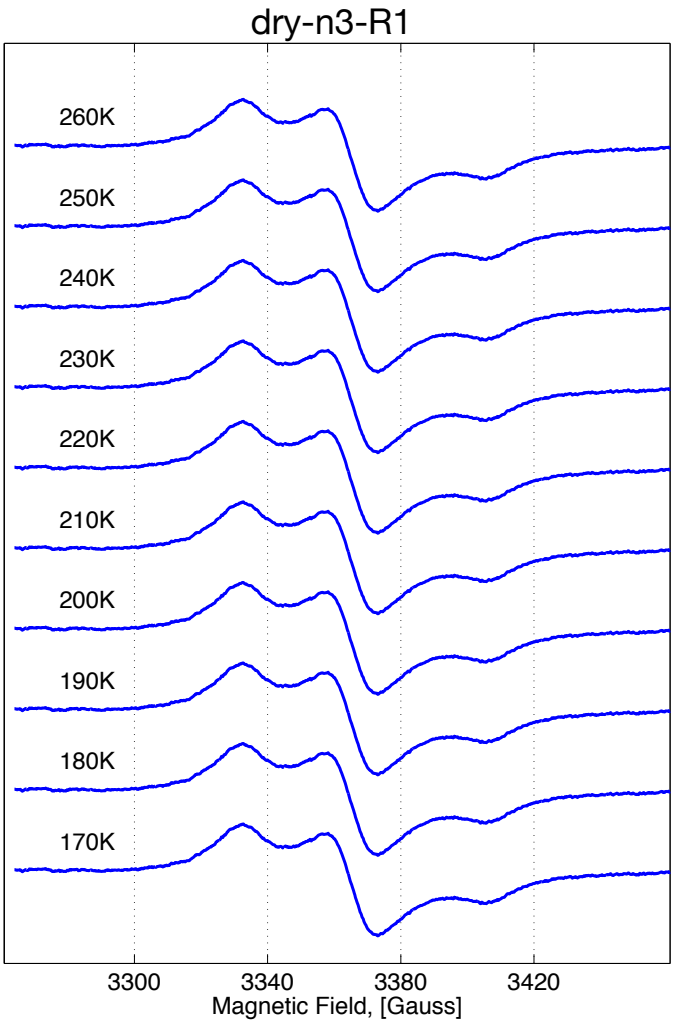

Figure S2. The cw-ESR spectra obtained for the dry n3-R1 in the studied temperature range between 170 ~ 260 K.

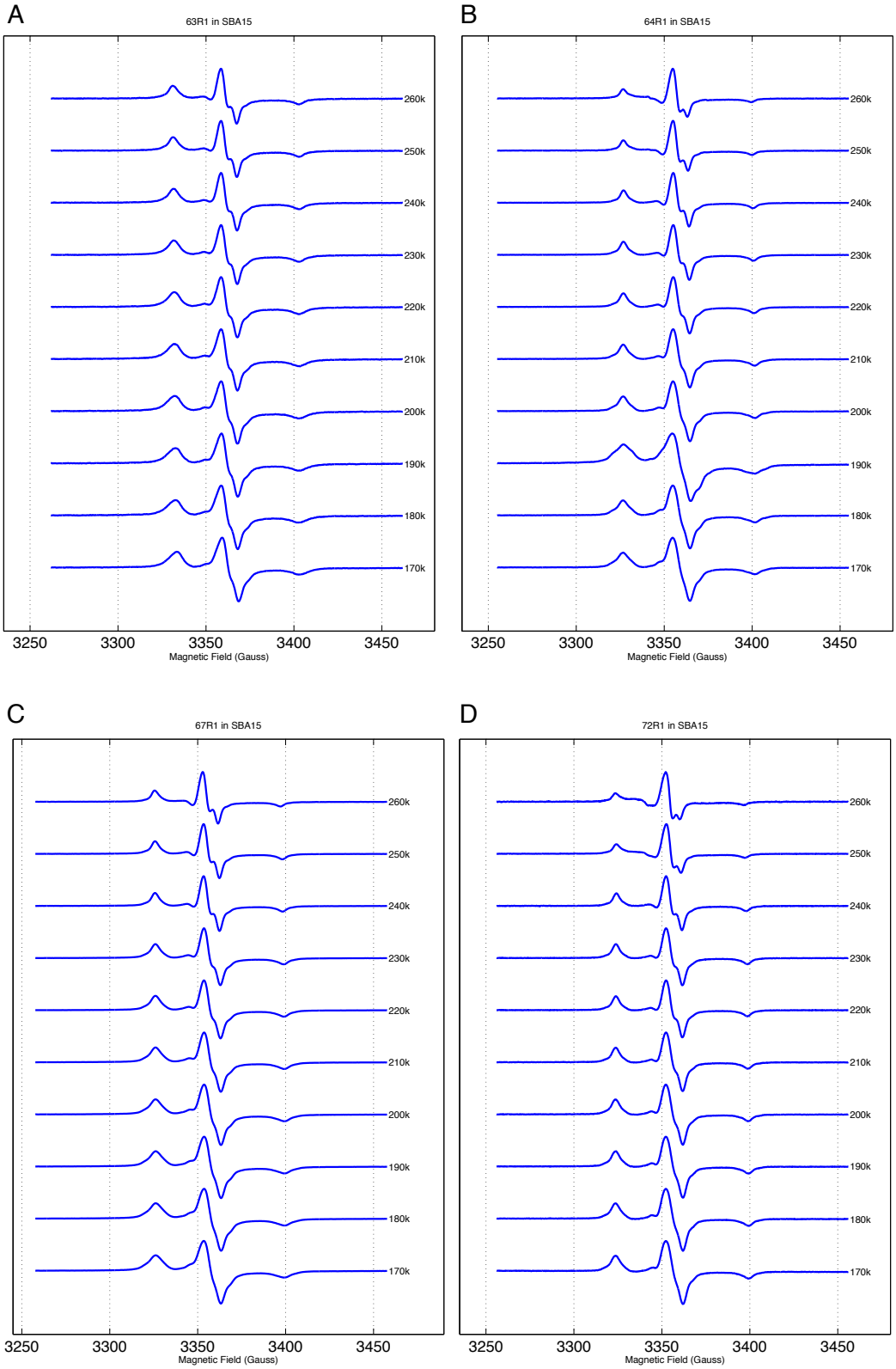

Figure S3. The cw-ESR spectra of the Bax proteins encapsulated in SBA15. They are the spectra of (A) Bax63R1, (B) Bax64R1, (C) Bax67R1, and (D) Bax72R1, at temperatures 170 ~ 260 K.

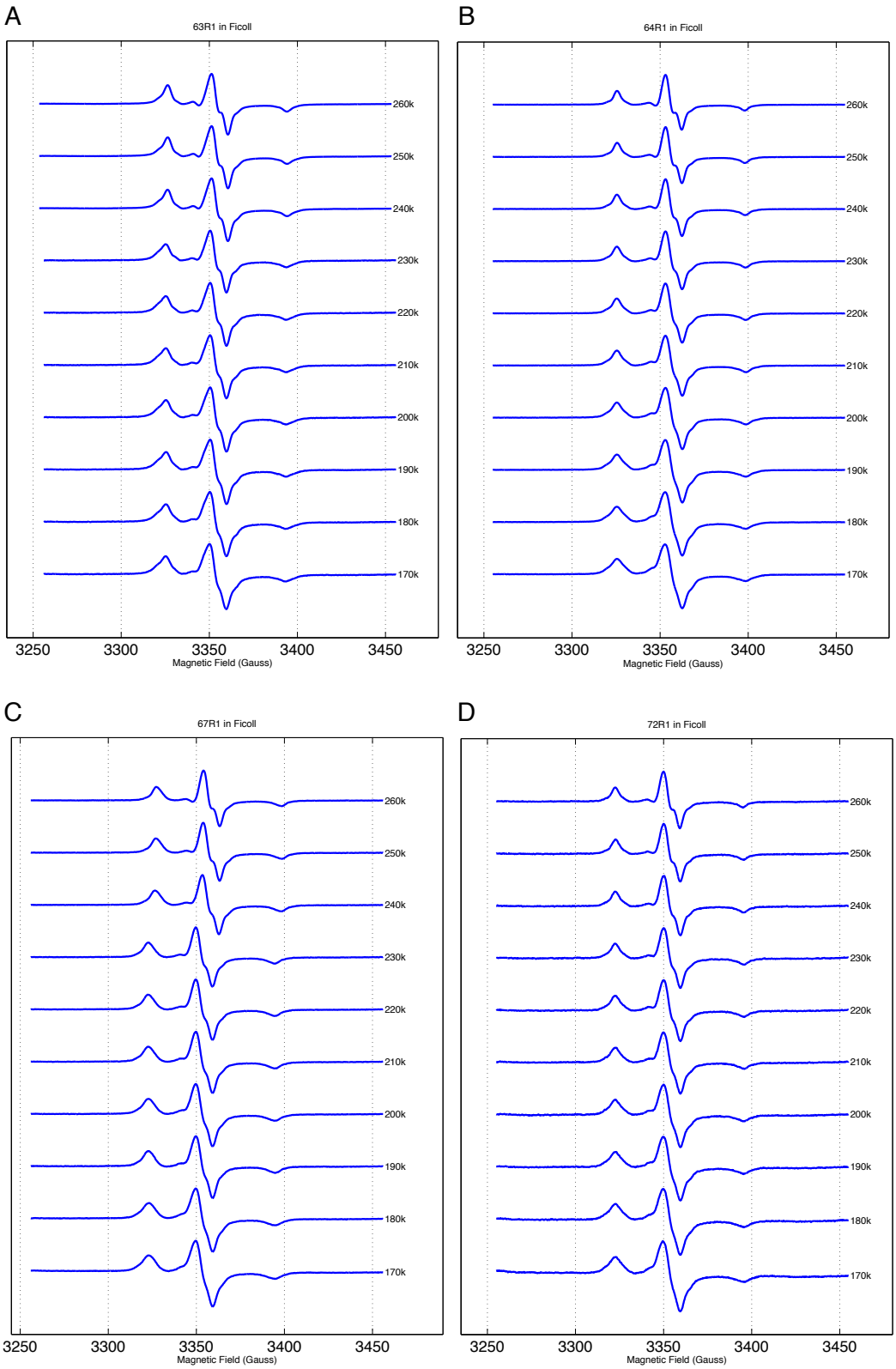

Figure S4. The cw-ESR spectra of the Bax proteins in the vitrified bulk solvent containing 40% (w/w) ficoll. They are the spectra of (A) Bax63R1, (B) Bax64R1, (C) Bax67R1, and (D) Bax72R1, at temperatures 170 ~ 260 K.

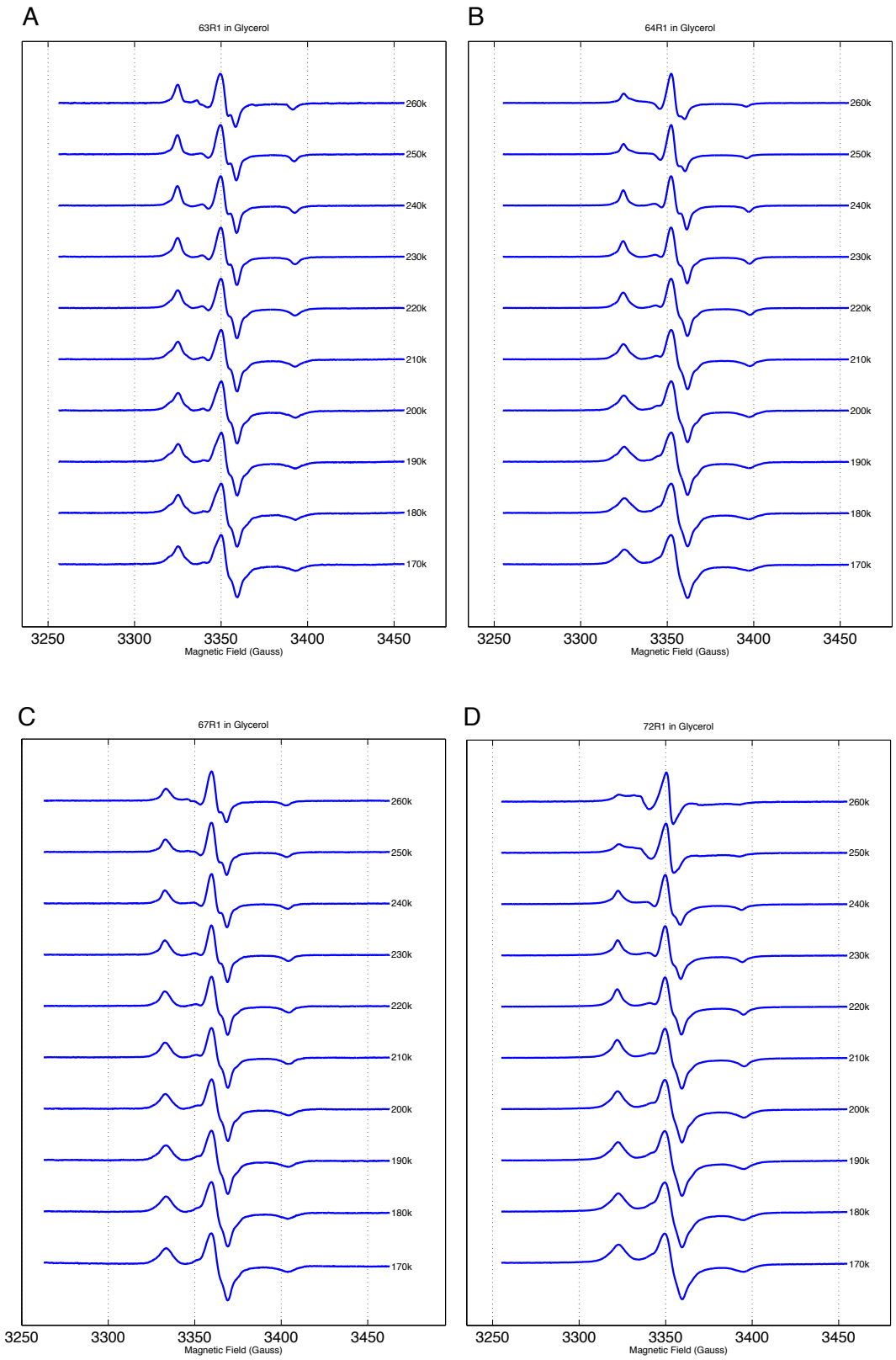

Figure S5. The cw-ESR spectra of the Bax proteins in the vitrified bulk solvent containing 40% (v/v) glycerol. They are the spectra of (A) Bax63R1, (B) Bax64R1, (C) Bax67R1, and (D) Bax72R1, at temperatures 170 ~ 260 K.

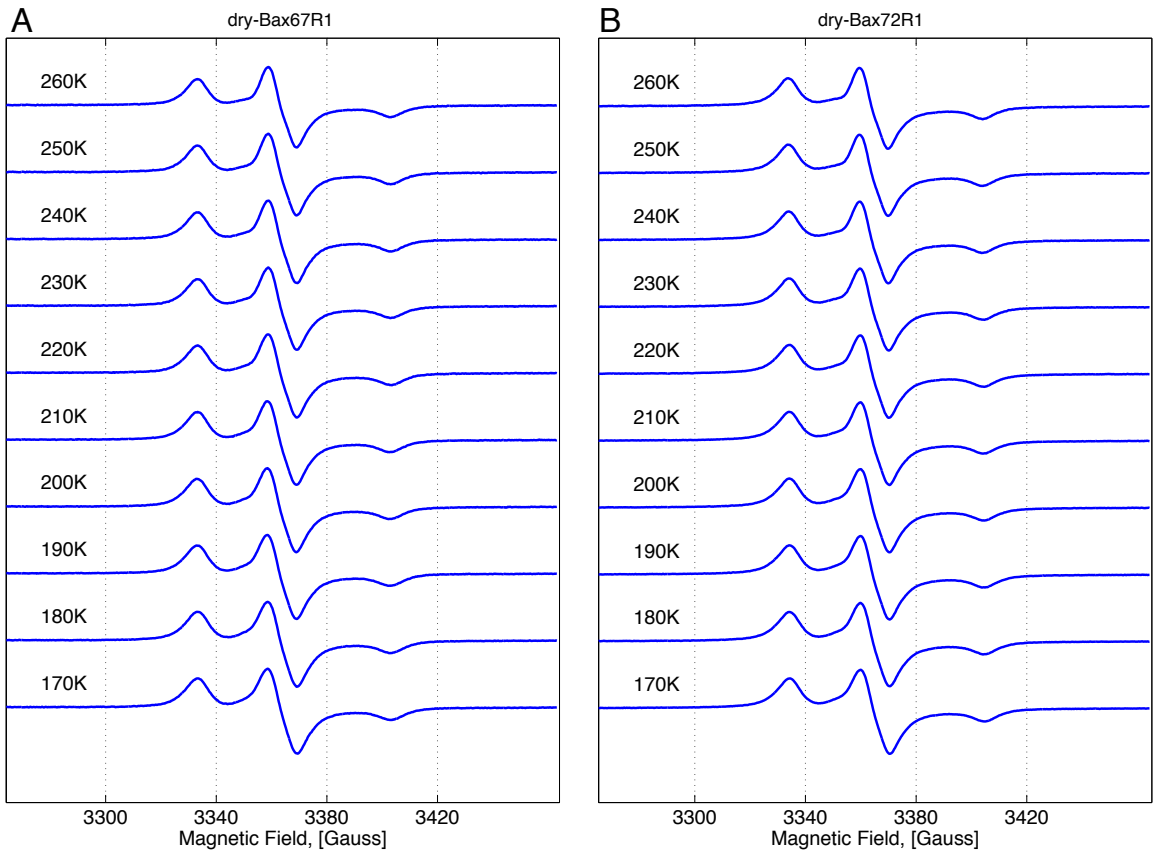

Figure S6. The cw-ESR spectra obtained for the dry Bax67R1 (A) and the dry Bax72R1 in the studied temperature range between 170 ~ 260 K.

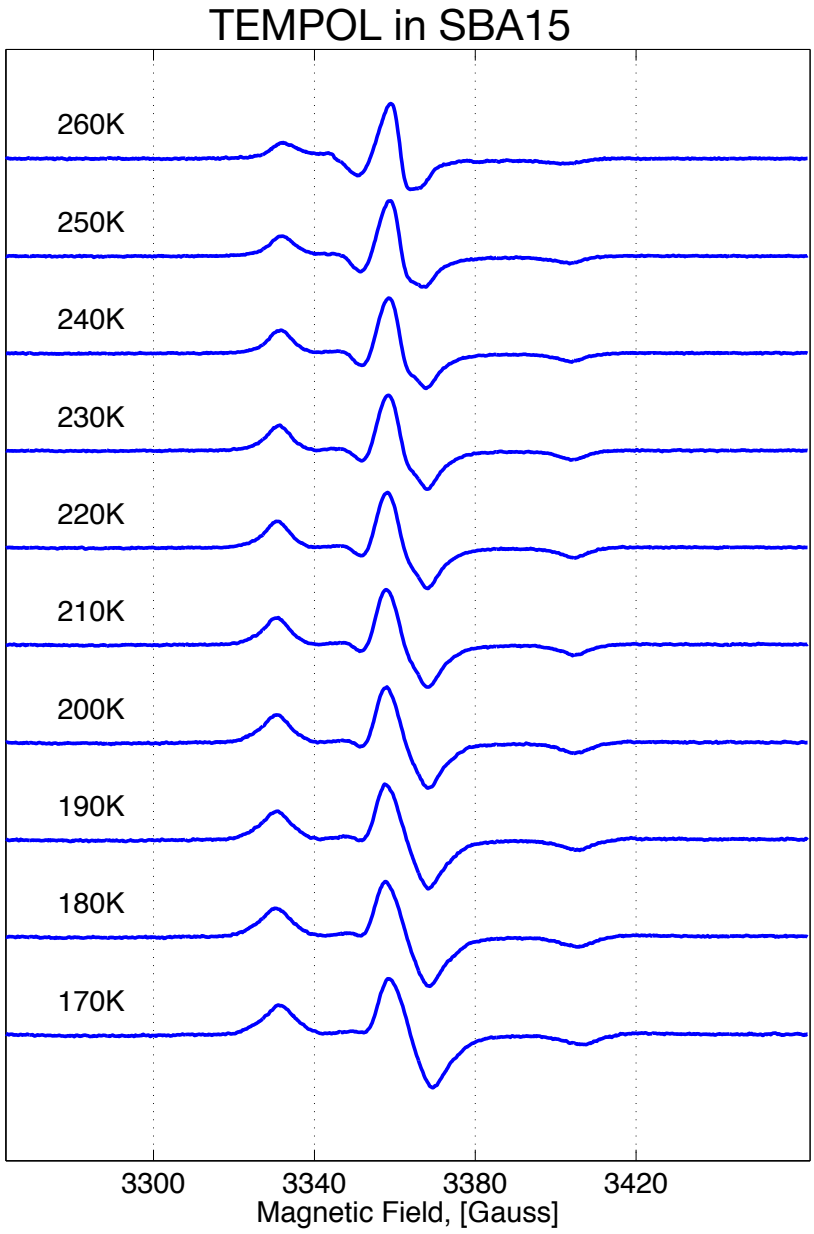

Figure S7. The cw-ESR spectra obtained for TEMPOL in SBA15 nanochannels containing protein buffer, i.e., the buffer A in Method. The corresponding $2A_{zz}$ values are (from high to low T) 68.9, 71.5, 72.5, 72.5, 74.2, 74.4, 74.4, 75.2, 75.8, 76.6 Gauss.

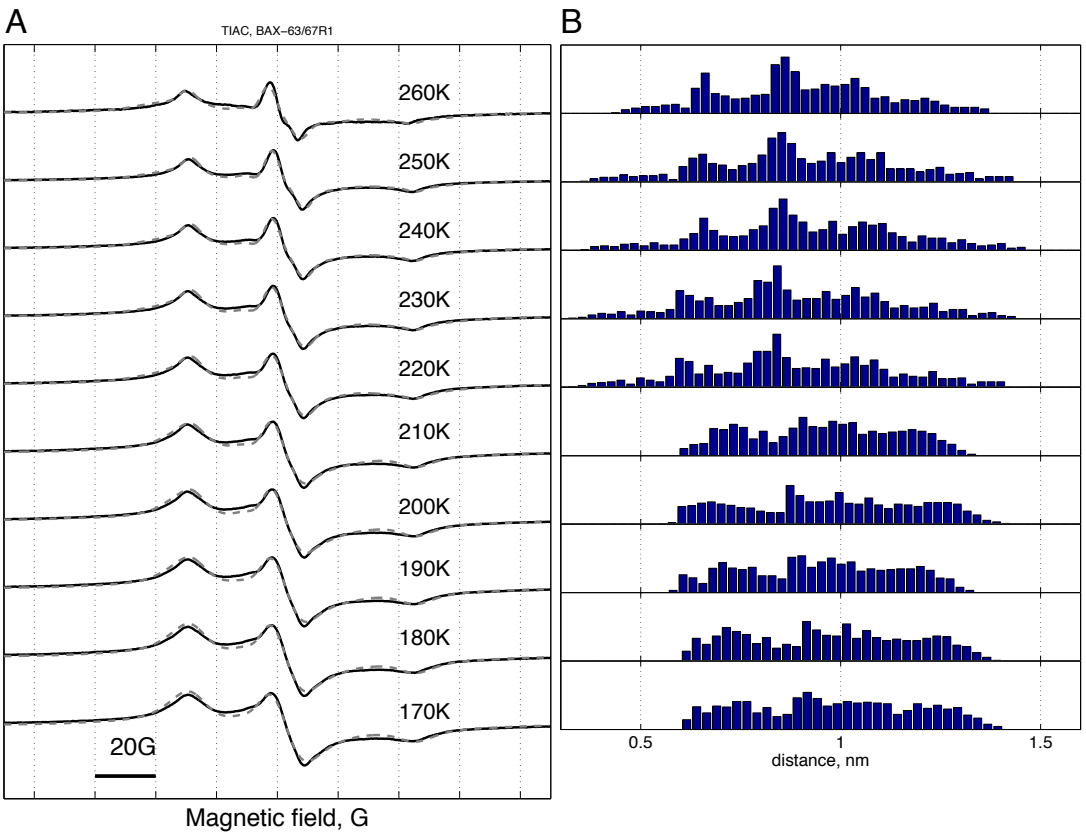

Figure S8. (A) The cw-ESR spectra of the doubly labeled Bax63/67R1 at temperatures 170 ~ 260 K are plotted in solid lines while the theoretical fits of the TIAC analysis to the experimental spectra are shown in dashed lines. (B) The histogram representing the inter-spin distance distributions P(r) concerning temperature.